

The Voronoi Diagram of Rotating Rays

With applications to Floodlight Illumination

Carlos Alegría ✉ 

Dipartimento di Ingegneria, Università Roma Tre, Rome, Italy

Ioannis Mantas ✉ 

Faculty of Informatics, Università della Svizzera italiana, Lugano, Switzerland

Evanthia Papadopoulou ✉ 

Faculty of Informatics, Università della Svizzera italiana, Lugano, Switzerland

Marko Savić ✉ 

Department of Mathematics and Informatics, Faculty of Sciences, University of Novi Sad, Serbia

Hendrik Schrezenmaier ✉

Institut für Mathematik, Technische Universität Berlin, Germany

Carlos Seara ✉

Departament de Matemàtiques, Universitat Politècnica de Catalunya, Barcelona, Spain

Martin Suderland ✉ 

Faculty of Informatics, Università della Svizzera italiana, Lugano, Switzerland

Abstract

We introduce the *Voronoi Diagram of Rotating Rays*, a Voronoi structure where the input sites are rays, and the distance function is the counterclockwise angular distance between a point and a ray-site. This novel Voronoi diagram is motivated by illumination and coverage problems, where a domain has to be covered by floodlights (wedges) of uniform angle, and the goal is to find the minimum angle necessary to cover the domain. We study the diagram in the plane, and we present structural properties, combinatorial complexity bounds, and a construction algorithm. If the rays are induced by a convex polygon, we show how to construct the ray Voronoi diagram within this polygon in linear time. Using this information, we can find in optimal linear time the *Brocard angle*, the minimum angle required to illuminate a convex polygon with floodlights of uniform angle. This last algorithm improves upon previous results, settling an interesting open problem.

2012 ACM Subject Classification Theory of computation → Computational geometry

Keywords and phrases rotating rays, Voronoi diagram, oriented angular distance, Brocard angle, floodlight illumination, coverage problems, art gallery problems

Digital Object Identifier 10.4230/LIPIcs.ESA.2021.5

Funding C.A. was supported by MIUR Proj. “AHeAD” n° 20174LF3T8. Early work of I.M. and E.P. were supported by the DACH project Voronoi++, SNF-200021E_154387. M.S. is partly supported by the Ministry of Education, Science and Technological Development of the Republic of Serbia (Grant No. 451-03-9/2021-14/200125), and the Provincial Secretariat for Higher Education and Scientific Research, Province of Vojvodina. Early work of H.S. was partly supported by the DFG grant FE-340/11-1. C.S. was supported by project PID2019-104129GB-I00/AEI/10.13039/501100011033. This project has received funding from the European Union’s Horizon 2020 research and innovation programme under the Marie Skłodowska-Curie grant agreement No 734922.

Acknowledgements Initial discussions took place at the Intensive Research Program in Discrete, Combinatorial and Computational Geometry in Barcelona, Spain, in 2018. We are grateful to the organizers for providing the platform to meet and collaborate.



© Carlos Alegría, Ioannis Mantas, Evanthia Papadopoulou, Marko Savić, Hendrik Schrezenmaier, Carlos Seara, and Martin Suderland;

licensed under Creative Commons License CC-BY 4.0

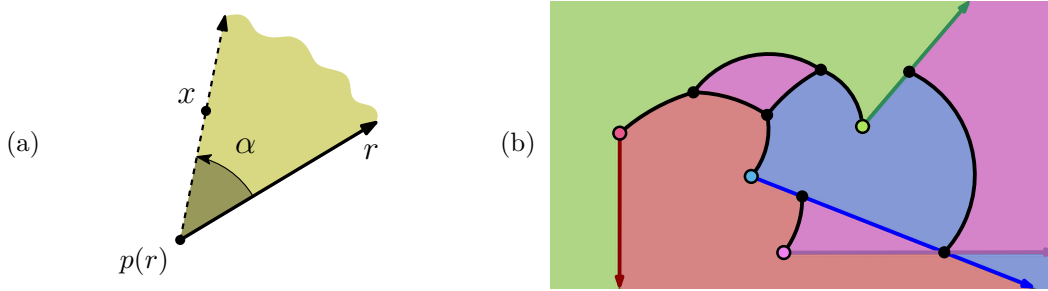
29th Annual European Symposium on Algorithms (ESA 2021).

Editors: Petra Mutzel, Rasmus Pagh, and Grzegorz Herman; Article No. 5; pp. 5:1–5:16

Leibniz International Proceedings in Informatics



Schloss Dagstuhl – Leibniz-Zentrum für Informatik, Dagstuhl Publishing, Germany



■ **Figure 1** (a) An α -floodlight aligned with a ray r , having apex $p(r)$. The angle α is the angular distance from a point x to r . (b) The Rotating Rays Voronoi diagram of four rays in the plane. Each region is represented by a different color, and all points in a region are first illuminated by the ray of the respective color.

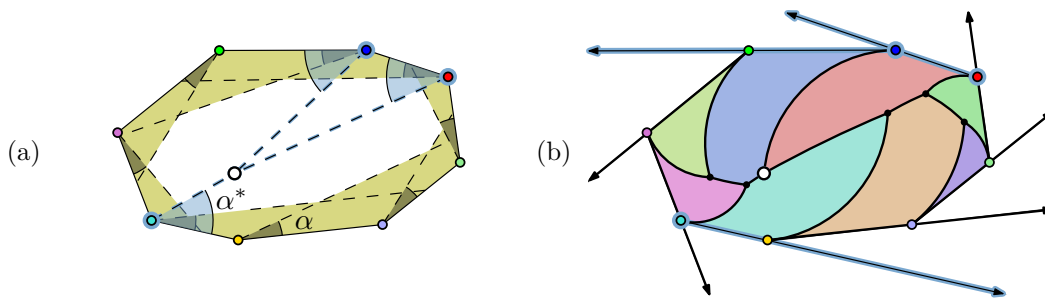
1 Introduction

In this work, we study the *Voronoi diagram of rotating rays* in the plane, which is defined by a set of n rays in \mathbb{R}^2 , under an angular distance function. Given a point x and a ray r in the plane, the *angular distance* from x to r is the smallest angle α such that, if we counterclockwise rotate r around its apex by α , it reaches (*illuminates*) x ; see Figure 1. We define this diagram and use it to solve related floodlight illumination problems.

Motivation. Illumination problems are well known *art gallery* type of problems, where a given domain has to be covered by so-called *floodlights*, which are light sources that illuminate a cone from their apex. The distance measure we study in this work is motivated by the following illumination problem. An α -*floodlight* is a floodlight with aperture α . Given a simple polygon P , an α -floodlight facing the interior of P is placed on each vertex v , in such a way that one of its rays contains the successor of v in the counterclockwise order of the vertices of P ; see Figure 2(a). The *Brocard Illumination problem* [1] asks for the *Brocard angle*, the smallest value of α for which the set of α -floodlights covers the interior of P .

When P is a convex polygon, the Brocard angle α^* can be revealed by constructing the Voronoi diagram of the rays placed at the vertices of P . In particular, α^* is realized at a vertex of the diagram with the maximum angular distance; see Figure 2(b). A rather natural extension is to follow a similar approach, not only in polygonal, but also in different domains. In addition to polygons, traditional domains to illuminate by floodlights include the entire plane, a region in the plane, or a single curve; see e.g., [6, 10, 25, 27]. Constructing the respective Voronoi diagram restricted to each domain yields the minimum angle needed by the floodlights to illuminate this domain. Hence, there is an interest in studying such Voronoi diagrams and in designing efficient construction algorithms for different domains.

Related work. In the Brocard illumination problem, a polygon P is called a *Brocard polygon*, if the Brocard angle is realized at a point, which is illuminated by all the floodlights, and is also equidistant to all the rays containing the sides of P [4]. The characterization of Brocard polygons has a long history, yet, only harmonic polygons (which include triangles and regular polygons) are known to be Brocard [7]. Nevertheless, we can detect if a convex polygon with n vertices is Brocard in $O(n)$ time, and compute the Brocard angle in such case in $O(1)$



■ **Figure 2** A polygon P . (a) Illumination by α -floodlights aligned with each edge of P . (b) The Voronoi diagram of the edge-aligned rays confined into P . Highlighted are the rays that realize the Brocard angle α^* , along with the point at which α^* is realized.

time. Algorithms for the computation of the Brocard angle of arbitrary simple polygons were recently presented by Alegría et al. [1]. The authors gave an $O(n^3 \log^2 n)$ time algorithm and complemented this with an $O(n \log n)$ -time algorithm for convex polygons¹.

Since their introduction [6], floodlight illumination problems have been studied a lot, see e.g., [22, 28]. The case when the floodlights are of uniform angle has also been explored by several authors, see e.g., [8, 13, 16, 23, 27]. From a different viewpoint, rotating α -floodlights can also be used to model devices with limited sensing range, like surveillance cameras or directional antennae; see [3, 9, 20, 21]. In this context, the minimum angle is interpreted as the minimum range needed by a set of devices to cover a domain. The Rotating Rays Voronoi Diagram is novel with respect to both the input sites and the distance function. A somewhat related diagram was defined in [11] to model dominance regions in the analysis of soccer matches [26].

Our contribution. We introduce the *Rotating Rays Voronoi Diagram* and prove a series of results, paving the way for future work on similar problems. Our interest in this diagram stems from its application to floodlight illumination in different domains.

- In Section 3, we consider the diagram in the plane. We identify structural properties which we complement with complexity results: an $\Omega(n^2)$ worst case lower bound and an $O(n^{2+\epsilon})$ upper bound. As a by-product we get an $O(n^{2+\epsilon})$ -time construction algorithm. This algorithm allows us to find, within the same time, the minimum angle needed to illuminate the plane with a given set of ray-aligned floodlights.
- Motivated by the Brocard illumination problem, in Section 4, we restrict our domain to a convex polygonal region bounded by the input set of sites. We study the Voronoi diagram in such domain and describe a construction algorithm that works in deterministic $\Theta(n)$ time. As our main contribution, we show how to use the resulting diagram to find the Brocard angle of a convex polygon in optimal linear time.
- Finally, in Section 5, we consider the case where the domain of interest is a curve, and we show how to construct the diagram along various types of curves.

¹ The $O(n)$ time analysis of the algorithm for convex polygons stated in [1] is not correct.

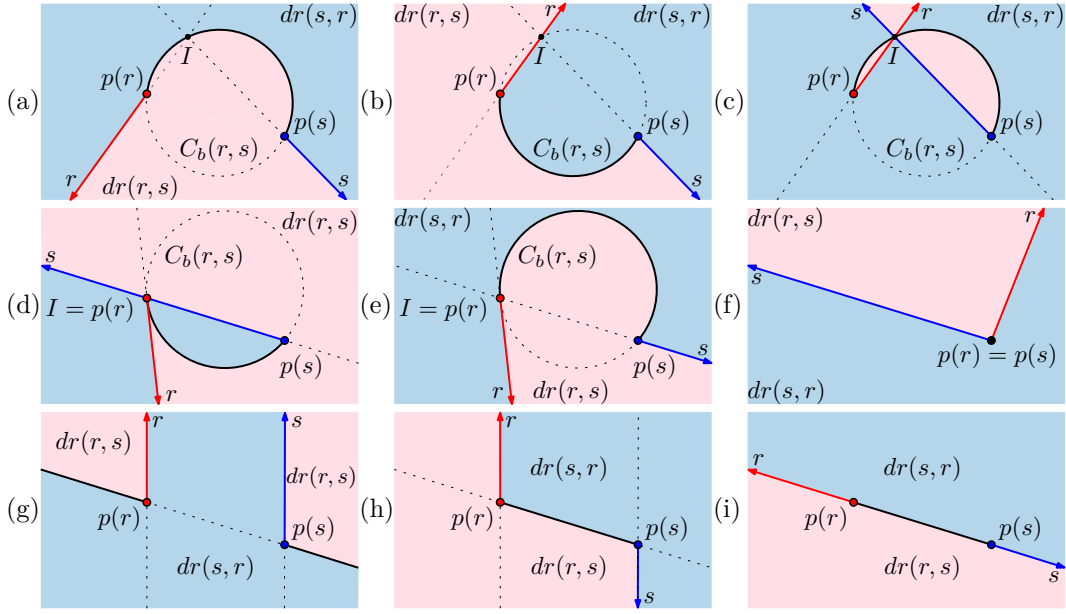


Figure 3 The bisector of two rays r and s , consisting of r (red ray), s (blue ray) and an arc of $C_b(r, s)$ (black curve), in different configurations. (a) Non-intersecting with $I \notin r \cup s$. (b) Non-intersecting with $I \in r$. (c) Intersecting. (d) “Tangent” with $p(r) \in s$. (e) “Tangent” with $p(r) \in l(s) \setminus s$. (f) Sharing their apex. (g) Parallel. (h) Anti-parallel with $l(r) \neq l(s)$. (i) Anti-parallel with $l(r) = l(s)$.

2 Preliminaries

Let \mathcal{S} be a set of n rays in \mathbb{R}^2 . Given a ray r , we denote its apex by $p(r)$, its supporting line by $l(r)$, and its direction in the unit circle by $\hat{d}(r)$. We define the distance function as follows.

► **Definition 1.** Given a ray r and a point $x \in \mathbb{R}^2$, the oriented angular distance from x to r , denoted by $d_{\angle}(x, r)$, is the minimum counterclockwise angle α from r to a ray with apex $p(r)$ passing through x ; see Figure 1(a). Further, we define $d_{\angle}(p(r), r) = 0$.

It is easy to see that the oriented angular distance is not a metric. Moreover, observe that $d_{\angle}(x, r) \in [0, 2\pi)$, and there is a discontinuity at 2π . Using this distance function, we define the bisector of two rays and the Voronoi diagram of a set of rays.

► **Definition 2.** Given two rays r and s , the dominance region of r over s , denoted by $dr(r, s)$, is the set of points with smaller angular distance to r than to s , i.e., $dr(r, s) := \{x \in \mathbb{R}^2 \mid d_{\angle}(x, r) < d_{\angle}(x, s)\}$. The angular bisector of r and s , denoted by $b_{\angle}(r, s)$, is the curve delimiting $dr(r, s)$ and $dr(s, r)$; see Figure 3.

Note that, due to the discontinuity of the distance function, our definition of a bisector is slightly different from standard, which is the locus of points equidistant from two sites.

Given two rays r and s , let $I = l(r) \cap l(s)$. The bisector $b_{\angle}(r, s)$ is the union of the two rays r and s , and a circular arc a that connects $p(r)$ to $p(s)$; see Figure 3. The arc a belongs to the bisecting circle $C_b(r, s)$, which we define as follows:

- If $I, p(r)$, and $p(s)$ are three distinct points, then $C_b(r, s)$ is the circle through $I, p(r)$, and $p(s)$. The arc a contains I , if and only if I lies either on none or on both of r and s ; see Figure 3(a), Figure 3(b) and Figure 3(c).

- If $I = p(r)$ and $I \neq p(s)$, then $C_b(r, s)$ is the circle tangent to $l(r)$ passing through $p(r)$ and $p(s)$. Both a and r lie on the same side of $l(s)$, if and only if $p(r)$ lies on s . We analogously define $C_b(r, s)$ if $I = p(s)$ and $I \neq p(r)$; see Figure 3(d) and Figure 3(e).
- If $p(r) = p(s)$, then both $C_b(r, s)$ and a degenerate to a single point; see Figure 3(f).
- If $l(r)$ and $l(s)$ are parallel, then $C_b(r, s)$ degenerates to the line through $p(r)$ and $p(s)$. If $\hat{d}(r) = -\hat{d}(s)$, then a is a line segment. If instead $\hat{d}(r) = \hat{d}(s)$, then a consists of two half-lines; see Figure 3(g), Figure 3(h) and Figure 3(i).

Observe that the oriented angular distance is monotone along the circular arc a . Further, the angular bisector is connected, unless its defining rays are parallel. For the sake of simplicity, unless otherwise stated, we assume that no two rays in \mathcal{S} have parallel supporting lines, and that the apex of any ray does not lie on any other ray.

► **Definition 3.** *The Rotating Rays Voronoi Diagram (RVD) of a set of rays \mathcal{S} is the subdivision of \mathbb{R}^2 into Voronoi regions defined as follows:*

$$vreg(r) := \{x \in \mathbb{R}^2 \mid \forall s \in \mathcal{S} \setminus \{r\} : d_{\angle}(x, r) < d_{\angle}(x, s)\}.$$

The graph structure of the diagram is $RVD(\mathcal{S}) := (\mathbb{R}^2 \setminus \bigcup_{r \in \mathcal{S}} vreg(r)) \cup \mathcal{S}$.

The Voronoi region $vreg(r)$ can be equivalently defined as the intersection of all the dominance regions of r , i.e., $vreg(r) = \bigcap_{s \in \mathcal{S} \setminus \{r\}} dr(r, s)$. A Voronoi region may be disconnected; each connected component of a Voronoi region is called a *face*.

The diagram $RVD(\mathcal{S})$ has different types of edges and vertices. An edge can be a line segment, a half-line, or a circular arc. A vertex can be the apex of a ray, the intersection point of two rays, the intersection point of three circular arcs, or the intersection point of a ray and a circular arc. Further, $RVD(\mathcal{S})$ is a planar graph with bounded maximum degree; thus, to bound its complexity, it suffices to bound any of its edges, vertices, or faces.

3 RVD in the Plane

In this section we study the diagram $RVD(\mathcal{S})$ in the plane. We first look at some properties and combinatorial complexity bounds. Then we consider the problem of illuminating the plane with a set of floodlights aligned with \mathcal{S} .

3.1 Properties, complexity, and an algorithm

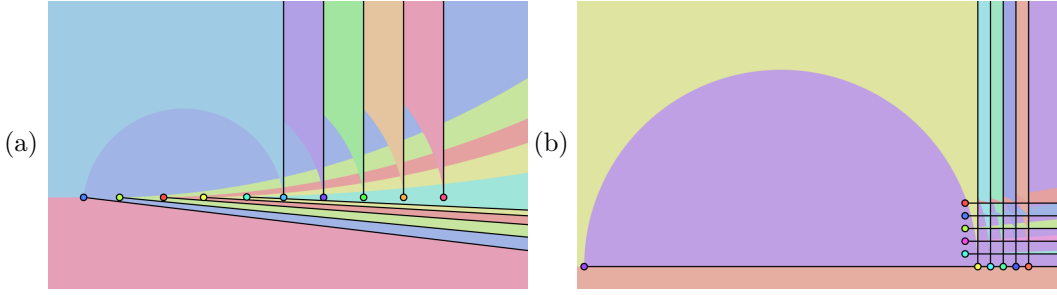
The diagram $RVD(\mathcal{S})$ satisfies the following two simple structural properties.

► **Lemma 4.** *$RVD(\mathcal{S})$ has exactly n unbounded faces, one for each ray in \mathcal{S} .*

Proof. Let r be an arbitrary ray of \mathcal{S} . To examine the unbounded portion of $vreg(r)$, consider the intersection of $RVD(\mathcal{S})$ with a circle Γ of sufficiently large radius, enclosing the vertices of $RVD(\mathcal{S})$ and the bisecting circles of all the bisectors of \mathcal{S} .

For $s \in \mathcal{S} \setminus \{r\}$, the intersection $dr(r, s) \cap \Gamma$ is a circular arc of Γ going counterclockwise from $r \cap \Gamma$ to $s \cap \Gamma$. The region $vreg(r)$ is the intersection of all the dominance regions of r , thus, $vreg(r) \cap \Gamma$ is the intersection of $n - 1$ circular arcs, all starting from r . Hence, $vreg(r) \cap \Gamma$ is a single arc starting from r and ending at the first ray on the counterclockwise ordering along Γ . So, for any ray r , the region $vreg(r)$ has exactly one unbounded face. ◀

► **Lemma 5.** *$RVD(\mathcal{S})$ is connected.*



■ **Figure 4** (a) A set of pairwise non-intersecting rays with $\text{RVD}(\mathcal{S})$ having $\Theta(n^2)$ complexity. (b) A diagram with a Voronoi region (purple ray - leftmost apex) having $\Theta(n^2)$ complexity.

Proof. Assume that $\text{RVD}(\mathcal{S})$ is not connected, hence, it has at least two connected components. Then some region $vreg(r)$ disconnects $\text{RVD}(\mathcal{S})$ by either having an unbounded face with two occurrences at infinity, or by enclosing a component creating conceptually an *island*.

The first case is excluded by the proof of Lemma 4. For the second case, consider the disconnected component of $\text{RVD}(\mathcal{S})$ surrounded by $vreg(r)$. This component consists of at least one face of a region $vreg(s)$ for some $s \in \mathcal{S}$. Then, in $\text{RVD}(\{r, s\})$, there is an island inside $vreg(r)$. Thus, $b_{\perp}(r, s)$ has a bounded connected component, in contradiction to the fact that each bisector is a single unbounded curve. ◀

We now study the combinatorial complexity of $\text{RVD}(\mathcal{S})$. An $\Omega(n^2)$ lower bound is easily achieved by a set \mathcal{S} of n pairwise intersecting rays. In such case, $\text{RVD}(\mathcal{S})$ has $\binom{n}{2} = \Theta(n^2)$ vertices (one per intersection of rays) and thus $\Omega(n^2)$ complexity. Next, we show that this bound also holds for pairwise non-intersecting rays.

► **Theorem 6.** *The worst case combinatorial complexity of $\text{RVD}(\mathcal{S})$ has an $\Omega(n^2)$ lower bound, even if the rays are pairwise non-intersecting.*

Proof. We give the following construction illustrated in Figure 4(a), where the Voronoi regions of the $n/2 - 1$ rays with the leftmost apices have $n/2 + 1$ faces each. We set $n = 2m$ and let $p(r_i) = (i, 0)$, $i = 1, \dots, 2m$, with rays r_{m+1}, \dots, r_{2m} pointing vertically upwards. For $i = 1, \dots, m$, let the direction of r_i be $\widehat{d}(r_i) = (\sin \alpha_i, \cos \alpha_i)$ with $\alpha_1 \in (3\pi/2, 2\pi)$ and $\alpha_i = \alpha_{i-1} + \epsilon_i$ where $\epsilon_i > 0$ for $i = 2, \dots, m$. We choose ϵ_i one by one, in the increasing order of i , so that both r_i and r_{i+1} have a face between any two consecutive upward shooting rays. This is always possible since we can choose ϵ_i small enough so that, at any x -coordinate $x < 2m$, the circular arc of $b_{\perp}(r_i, r_{i+1})$ is arbitrarily close to the x -axis and, thus, it is below the circular arc of $b_{\perp}(r_{i-1}, r_i)$. ◀

► **Theorem 7.** *A Voronoi region of $\text{RVD}(\mathcal{S})$ has $\Theta(n^2)$ complexity in the worst case.*

Proof. We first argue that the complexity of a region is $O(n^2)$. A vertex v of $\text{RVD}(\mathcal{S})$ can be defined by a triplet of rays $r, s, t \in \mathcal{S}$. The bisectors $b_{\perp}(r, s)$ and $b_{\perp}(r, t)$ intersect $O(1)$ times, hence, $\text{RVD}(\{r, s, t\})$ has $O(1)$ vertices. Now consider a ray r and its region $vreg(r)$. All but at most $O(n)$ vertices on the boundary of $vreg(r)$ are defined by r and a pair of sites. There are $\Theta(n^2)$ pairs, each inducing $O(1)$ vertices on $vreg(r)$, so $vreg(r)$ has $O(n^2)$ vertices.

We now give a construction of $n = 2m + 1$ rays, where a single region has $\Theta(n^2)$ complexity; refer to the construction of Figure 4(b). We first create a grid structure. For $i = 1, \dots, m$, let r_i be a ray with $p(r_i) = (i, 0)$ shooting vertically upward, and let s_i be a ray with $p(s_i) = (0, i)$ shooting horizontally to the right. For all $(i, j) \in \{1, \dots, m - 1\}^2$,

let $R(i, j)$ be the square $[i, i + 1) \times [j, j + 1)$. Each square $R(i, j)$ is made up of two faces of $\text{RVD}(\{r_1, \dots, r_m, s_1, \dots, s_m\})$, one belonging to $\text{vreg}(r_i)$ and one belonging to $\text{vreg}(s_j)$. Now let $\alpha(i, j) := \max\{\min\{d_{\angle}(x, r_i), d_{\angle}(x, s_j)\} \mid x \in R(i, j)\}$ and let $\alpha_{\min} := \min\{\alpha(i, j) \mid (i, j) \in \{1, \dots, m - 1\}^2\}$. It is easy to see that $\alpha_{\min} < \arctan 1/(m - 1)$.

We now introduce another ray t , so that $\max\{d_{\angle}(x, t) \mid x \in [1, n - 1]^2\} < \alpha_{\min}$. This can be achieved if $p(t) = (-n^2, 0)$ and t is shooting horizontally to the right. This means that in each $R(i, j)$, for $(i, j) \in \{1, \dots, n - 1\}^2$, t will visit some point before any of the rays r_i or s_j , implying that $\text{vreg}(t)$ has $\Theta(n^2)$ faces. ◀

We now show how the angular distance function can be adapted in order to apply the general upper bounds of Sharir [24]. As a by-product we also obtain an algorithm for $\text{RVD}(\mathcal{S})$.

► **Theorem 8.** *$\text{RVD}(\mathcal{S})$ has $O(n^{2+\epsilon})$ combinatorial complexity, for any $\epsilon > 0$. Further, $\text{RVD}(\mathcal{S})$ can be constructed in $O(n^{2+\epsilon})$ time.*

Proof. Each site r induces a function $d_{\angle}^r(x) = d_{\angle}(x, r)$ which maps a point $x = (x_1, x_2) \in \mathbb{R}^2$ to its angular distance from r . The RVD can be seen as the projection of the lower envelope of the graphs of these distance functions in 3-space to the plane. For algebraic distance functions, Sharir [24] gives complexity bounds for this lower envelope accompanied with algorithmic results. The angular distance functions though are not algebraic. Our strategy is to find algebraic functions d_{alg}^r that are equivalent to the functions d_{\angle}^r for the computation of the lower envelope, i.e., they fulfill the following property for all $r, s \in \mathcal{S}$ and $x \in \mathbb{R}^2$:

$$d_{\angle}^r(x) < d_{\angle}^s(x) \Leftrightarrow d_{\text{alg}}^r(x) < d_{\text{alg}}^s(x).$$

Without loss of generality, assume that $p(r)$ lies on the origin and r is facing to the right, that is, in the positive x_1 -direction of the coordinate system. Let $x \in \mathbb{R}^2$ and $\alpha := d_{\angle}^r(x)$. Then we want to set $d_{\text{alg}}^r(x) := 1 - \cos(\alpha)$ if $0 \leq \alpha \leq \pi$, and $d_{\text{alg}}^r(x) := 3 + \cos(\alpha)$ if $\pi < \alpha < 2\pi$. The function $x \mapsto \cos(\alpha)$ is indeed algebraic since it is obtained by first scaling x to unit length and then mapping it to its first coordinate. Then we have

$$d_{\text{alg}}^r(x) = \begin{cases} 0 & \text{if } x_1 = x_2 = 0, \\ 1 - \frac{x_1}{\sqrt{x_1^2 + x_2^2}} & \text{if } x_1 \neq 0, x_2 \geq 0, \\ 3 + \frac{x_1}{\sqrt{x_1^2 + x_2^2}} & \text{otherwise.} \end{cases}$$

Since d_{alg}^r consists of three patches, which are all algebraic and have simple domain boundaries, applying [24] to these functions yields the claimed results. ◀

3.2 Minimum angle needed to illuminate the plane

Given a set \mathcal{S} of n rays in \mathbb{R}^2 , the Brocard Illumination problem can be naturally extended to the plane as follows. An α -floodlight f is *aligned with* a ray r , if f is equal to r when $\alpha = 0$. Let f_r denote a floodlight aligned with the ray $r \in \mathcal{S}$. The goal is to find the minimum angle α^* for which the set of α^* -floodlights $\{f_r \mid r \in \mathcal{S}\}$ illuminates the entire plane.

The angle α^* is realized at a point x^* that has the maximum angular distance to its nearest ray, that is, $\alpha^* = \max_{x \in \mathbb{R}^2} \min_{r \in \mathcal{S}} d_{\angle}(x, r)$. Hence, the point x^* necessarily lies on $\text{RVD}(\mathcal{S})$. Since the distance along a circular edge is monotone, it follows that x^* cannot lie on such an edge. Thus, x^* is either a vertex of $\text{RVD}(\mathcal{S})$ or a point at infinity on a ray of \mathcal{S} . We can find x^* , and hence α^* , by first constructing $\text{RVD}(\mathcal{S})$ in $O(n^{2+\epsilon})$ time, and then traversing the diagram in linear time in its size. We obtain the following result.

► **Theorem 9.** Given a set of rays \mathcal{S} and an α -floodlight aligned with each ray, the minimum angle α^* needed to illuminate \mathbb{R}^2 can be found in $O(n^{2+\epsilon})$ time, for any $\epsilon > 0$.

Next, we give tight bounds on the value of α^* .

► **Proposition 10.** Given a set of rays \mathcal{S} and an α -floodlight aligned with each ray, the angle α^* is greater or equal to $2\pi/n$. Further, α^* can take any value in the interval $[2\pi/n, 2\pi)$.

Proof. For the lower bound, consider that in order to illuminate the entire plane, all the points at infinity should also be illuminated. To illuminate these points, the sum of the angles of all rays, should be at least 2π . Hence, in the best case, each point at infinity is seen by exactly one ray, and the $2\pi/n$ lower bound follows. Next, we give a construction realizing this bound.

Let \mathcal{S} be a set of rays having their apices on $(0,0)$, with the property that any two consecutive rays have an angular difference of $2\pi/n$. The last points to be illuminated will be all the points on the right side of each ray r_i . These points are illuminated simultaneously by r_{i-1} when α reaches $2\pi/n$. Further, this construction can be easily adapted to attain any value in $(2\pi/n, 2\pi)$, by expanding a wedge bounded by two consecutive rays to the desired angle and shrinking all the other wedges analogously. ◀

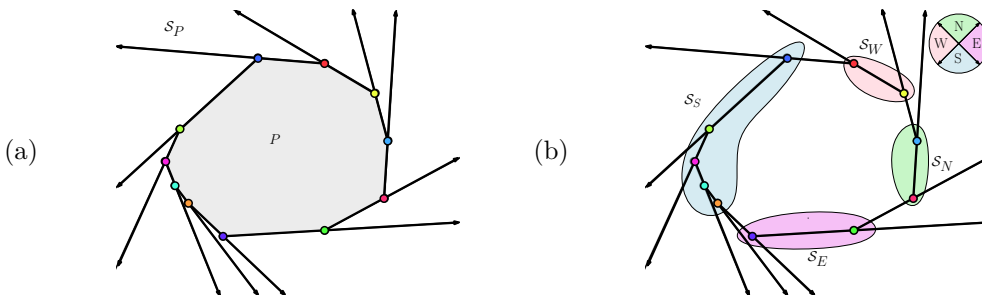
4 RVD of a convex polygon: Brocard illumination

We now turn our attention to the Brocard illumination problem. We are given a convex polygon P with n vertices, and we want to find the Brocard angle α^* of P . By computing an RVD restricted to P , we show how to compute α^* in optimal $\Theta(n)$ time.

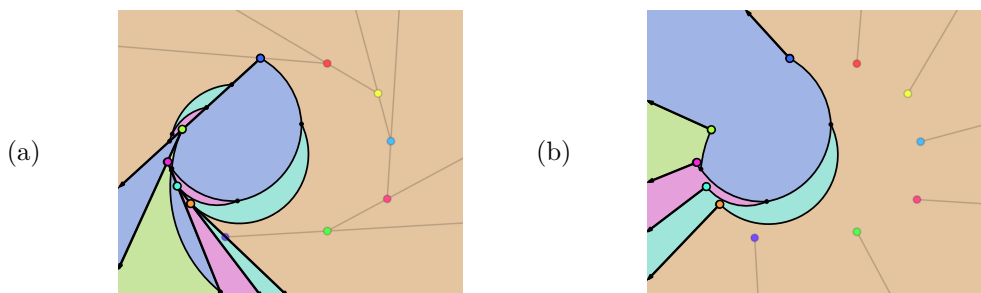
Let \mathcal{S}_P be the set of n rays such that each ray has a vertex $v \in P$ as apex, and passes through the successor vertex of v in a counterclockwise traversal of P ; see Figure 5(a). Let $\text{PRVD}(\mathcal{S}_P)$ be the diagram $\text{RVD}(\mathcal{S}_P)$ restricted to the interior of P . We first describe an algorithm to construct $\text{PRVD}(\mathcal{S}_P)$ and then show to use this diagram to obtain α^* . Note that we do not construct the complete $\text{RVD}(\mathcal{S}_P)$, which may have $\Theta(n^2)$ complexity, but only $\text{PRVD}(\mathcal{S}_P)$, which has $\Theta(n)$ size.

4.1 Algorithm to compute RVD of a convex polygon

The general strategy is to split the problem into four subproblems. Each subproblem will satisfy a set of conditions that allows us to use the existing $\Theta(n)$ time algorithms, which are based on *abstract Voronoi diagrams* [17, 19]. We then complete our construction by merging the resulting diagrams.



■ **Figure 5** (a) A convex polygon P and the corresponding set of rays \mathcal{S}_P . (b) The partitioning of \mathcal{S}_P into the four subsets $\mathcal{S}_N, \mathcal{S}_W, \mathcal{S}_S$ and \mathcal{S}_E , depending on the direction of the rays.



■ **Figure 6** (a) The diagram $\text{RVD}(\mathcal{S}_S)$; some Voronoi regions are disconnected. (b) The diagram $\text{RVD}(\mathcal{S}_S^r)$, after a clockwise rotation of $\pi/2$; all Voronoi regions are connected.

More specifically, we first partition \mathcal{S}_P into four sets $\mathcal{S}_N, \mathcal{S}_W, \mathcal{S}_S$ and \mathcal{S}_E depending whether a ray points north, west, south or east respectively; see Figure 5(b). In this way, rays in a subset are consecutive and the direction of any two rays have a difference of at most $\pi/2$. For each set \mathcal{S}_d , $d \in \{N, W, S, E\}$, we obtain a set \mathcal{S}_d^r in which every ray of \mathcal{S}_d is rotated clockwise by an angle of $\pi/2$; see Figure 6. Then, we construct each diagram $\text{RVD}(\mathcal{S}_d^r)$ independently. Finally, we merge the four diagrams to obtain $\text{PRVD}(\mathcal{S}_P)$; see Figure 8.

4.2 The four diagrams of \mathcal{S}_d^r

To construct the diagram of each subset \mathcal{S}_d^r in $\Theta(|\mathcal{S}_d^r|)$ time, we make use of the *abstract Voronoi diagrams* framework [17, 18]. To fall under this framework, the system of angular bisectors must satisfy the following three *axioms*:

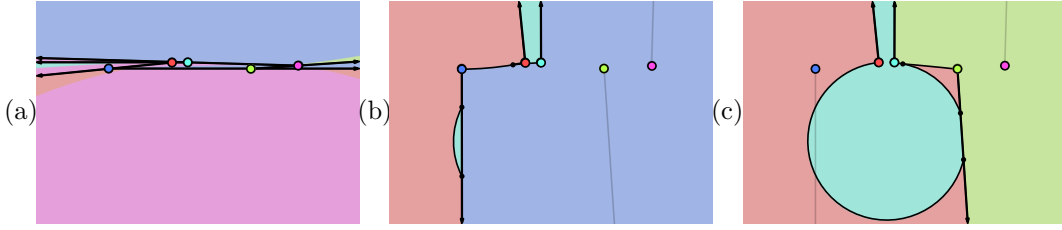
- **(A1)** The bisector $b_{\angle}(r, s)$, $\forall r, s \in \mathcal{S}$, is an unbounded Jordan curve.
- **(A2)** The region $\text{vreg}(r)$ in $\text{RVD}(\mathcal{S}')$, $\forall \mathcal{S}' \subseteq \mathcal{S}$ and $\forall r \in \mathcal{S}'$, is non-empty and connected.
- **(A3)** The closure of the union of all regions in $\text{RVD}(\mathcal{S}')$, $\forall \mathcal{S}' \subseteq \mathcal{S}$, covers \mathbb{R}^2 .

► **Lemma 11.** *The system of bisectors of \mathcal{S}_d^r satisfies the axioms (A1)-(A3).*

Proof sketch. (A1): Consider a pair of rays $r, s \in \mathcal{S}_d^r$. Let ℓ be the line through $p(r)$ and $p(s)$. Let $x \neq p(r)$ and $y \neq p(s)$ denote respectively, two points lying on r and s . Observe that the angles $\angle(p(s), p(r), x)$, $\angle(x, p(r), p(s))$, $\angle(y, p(s), p(r))$, and $\angle(p(r), p(s), y)$ are all greater than or equal to $\frac{\pi}{2}$, where $\angle(x, y, z)$ denotes the counterclockwise angle at point y , between the rays with apex y passing through x and z , respectively. Hence, r and s are non-intersecting regardless of whether both are contained on ℓ , or lie on the same side of ℓ . The bisector of two non-intersecting rays is an unbounded Jordan curve.

(A2): A Voronoi region $\text{vreg}(r)$ is obviously non-empty as it contains the ray r . Regarding the region connectivity, we claim that no ray of \mathcal{S}_d^r cuts twice a bisecting circle induced by the rays of \mathcal{S}_d^r . From the analysis of Section 2, this implies that every region of $\text{RVD}(\mathcal{S}_d^r)$ is connected, since it consists of a single unbounded face. Consider three rays $r, s, t \in \mathcal{S}_d$. The angle $-\alpha$ required to rotate r around $p(r)$ such that $l(r)$ is either tangent to or not intersecting $C_b(s, t)$ is strictly greater than $-\frac{\pi}{2}$. After rotating r by $-\frac{\pi}{2} \in [-\alpha, -(\alpha + \pi)]$, we obtain a ray in \mathcal{S}_d^r that does not intersect twice $C_b(r, s)$; see Figure 6(b). Our claim follows since \mathcal{S}_d and \mathcal{S}_d^r induce the same set of bisecting circles.

(A3): The diagram $\text{RVD}(\mathcal{S}_d^r)$ is defined by distance functions, one for each site in \mathcal{S}_d^r , whose domain is the entire plane. Thus, it follows that any point in the plane belongs to the closure of a region of $\text{RVD}(\mathcal{S}_d^r)$. ◀



■ **Figure 7** (a) $\text{RVD}(\mathcal{S}_P)$ of a polygon with five vertices. (b) A subset of three rays rotated by $-\pi/2$. The teal region has two faces; for it to be connected, the rays should be rotated by an angle greater than $-\pi/2$. (c) A subset of three rays rotated by $-\pi/2$. The red region has two faces; for it to be connected, the rays should be rotated by an angle smaller than $-\pi/2$.

Since each Voronoi region is connected, and it has exactly one unbounded face, as shown in Lemma 4, it follows that $\text{RVD}(\mathcal{S}_d^r)$ is a tree of complexity $\Theta(\mathcal{S}_d^r)$.

It is worth to note that the original set \mathcal{S}_P need not satisfy axioms (A1)-(A3), thus, $\text{RVD}(\mathcal{S}_P)$ need not fall under the framework of abstract Voronoi diagrams, and hence, the partition into the four subsets and the rotation.

The intuition behind the rotation of the rays comes from the fact that only circular parts of bisectors appear in $\text{PRVD}(\mathcal{S}_P)$, and that the bisecting circles remain the same under a uniform rotation. The partitioning of \mathcal{S}_P into the specific four sets is justified by the following remark.

► **Remark 12.** There are sets of rays \mathcal{S}_P for which there exists no unique angle to rotate the rays in \mathcal{S}_P , so that (A2) is satisfied. Refer to Figure 7.

$\text{RVD}(\mathcal{S}_d^r)$ can be constructed in $O(n \log n)$ time [17]. We can construct $\text{RVD}(\mathcal{S}_d^r)$ in $O(n)$ time by showing that the system of bisectors of \mathcal{S}_d^r falls under the *Hamiltonian abstract Voronoi diagram* framework of Klein and Lingas [19]. In addition to satisfying (A1)-(A3), the *cyclic version* of [19] requires the following axiom to be satisfied:

- **(A4)** There exists a Jordan curve \mathcal{H} of constant complexity such that, \mathcal{H} visits the region $\text{vreg}(r)$ in $\text{RVD}(\mathcal{S}')$, $\forall \mathcal{S}' \subseteq \mathcal{S}$ and $\forall r \in \mathcal{S}'$, exactly once.

If a Voronoi diagram satisfies axioms (A1)-(A4) and the ordering of the regions of $\text{RVD}(\mathcal{S}')$ along \mathcal{H} is given, then $\text{RVD}(\mathcal{S})$ can be computed in $\Theta(n)$ -time [19]. Hence, it suffices to find a curve \mathcal{H} satisfying these properties. We show this in the following.

► **Lemma 13.** $\text{RVD}(\mathcal{S}_d^r)$ can be constructed in deterministic $\Theta(|\mathcal{S}_d^r|)$ time.

Proof. We show that \mathcal{S}_d^r satisfies axiom (A4) of the Hamiltonian abstract Voronoi diagram framework [19]. The linear time algorithm is then a direct corollary of the existing results [19].

Let Γ be a circle of sufficient large radius enclosing all bisecting circles. Γ is obviously a Jordan curve of constant complexity. For any $\mathcal{S}' \subseteq \mathcal{S}_d^r$, the diagram $\text{RVD}(\mathcal{S}')$ is a tree, and by definition, Γ does not intersect any bisecting circle, hence, Γ visits each region of $\text{RVD}(\mathcal{S}')$ exactly once, with a change on the visited region happening when Γ intersects a ray. Γ is a Hamiltonian curve \mathcal{H} satisfying axiom (A4).

The ordering of the unbounded faces of $\text{RVD}(\mathcal{S}_d^r)$ corresponds to the ordering of the respective vertices along the polygon P , and this is maintained for any $\mathcal{S}' \subset \mathcal{S}_d^r$. The ordering of the vertices of P is given, so this concludes the proof. ◀

4.3 Merging the four diagrams

We now merge all the diagrams to obtain $\text{PRVD}(\mathcal{S}_P)$. Our merging procedure consists of two steps; see Figure 8. In an initial step we merge $\text{RVD}(\mathcal{S}_W^r)$ with $\text{RVD}(\mathcal{S}_S^r)$ to obtain $\text{RVD}(\mathcal{S}_W^r \cup \mathcal{S}_S^r)$, and analogously we obtain $\text{RVD}(\mathcal{S}_E^r \cup \mathcal{S}_N^r)$. Then, in a final step we merge the diagrams $\text{RVD}(\mathcal{S}_W^r \cup \mathcal{S}_S^r)$ and $\text{RVD}(\mathcal{S}_E^r \cup \mathcal{S}_N^r)$, restricted to the interior of P , to obtain $\text{PRVD}(\mathcal{S}_P)$. We show the following statement.

► **Lemma 14.** *Given $\text{RVD}(\mathcal{S}_d)$, for all $d \in \{N, W, S, E\}$, $\text{PRVD}(\mathcal{S}_P)$ can be constructed in $\Theta(n)$ time.*

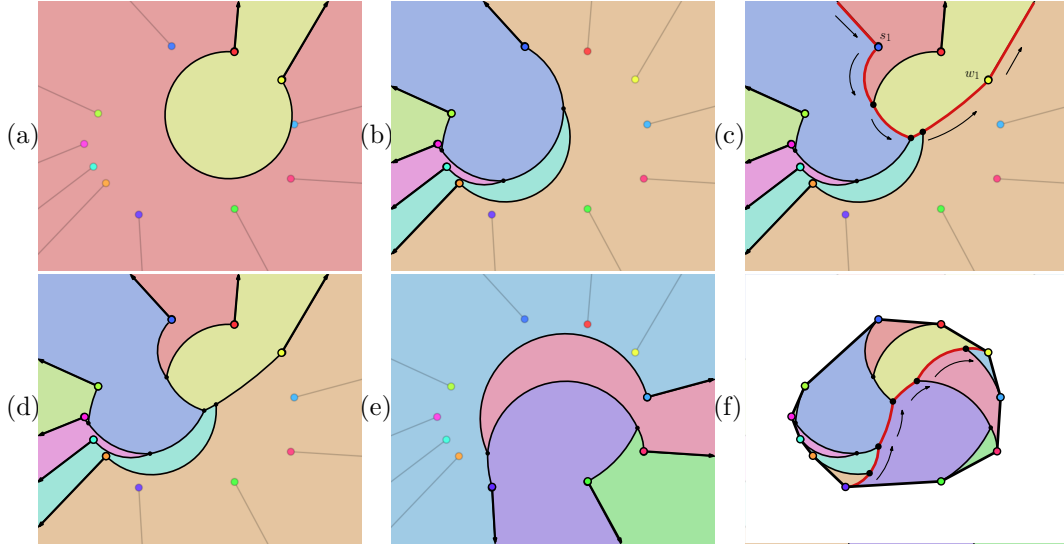
We now describe the two merging steps and sketch the arguments of the proof. Refer also to Figure 8 and Figure 9. Note that, although the four Voronoi diagrams $\text{RVD}(\mathcal{S}_d)$ to be merged fall under the abstract Voronoi framework, this is not the case for the resulting diagrams. This requires special care in the merging process.

Initial step. We describe how to merge $\text{RVD}(\mathcal{S}_W^r)$ with $\text{RVD}(\mathcal{S}_S^r)$. Let w_1, \dots, w_k be the rays in \mathcal{S}_W^r and let s_1, \dots, s_l be the rays in \mathcal{S}_S^r , as they appear ordered on P . We need to construct the *merge curve*, which consists of the rays s_1, w_1 and the set of circular edges of $\text{RVD}(\mathcal{S}_W^r \cup \mathcal{S}_S^r)$ equidistant to sites $w \in \mathcal{S}_W^r$ and $s \in \mathcal{S}_S^r$, which we denote by E_C . We describe each procedure separately.

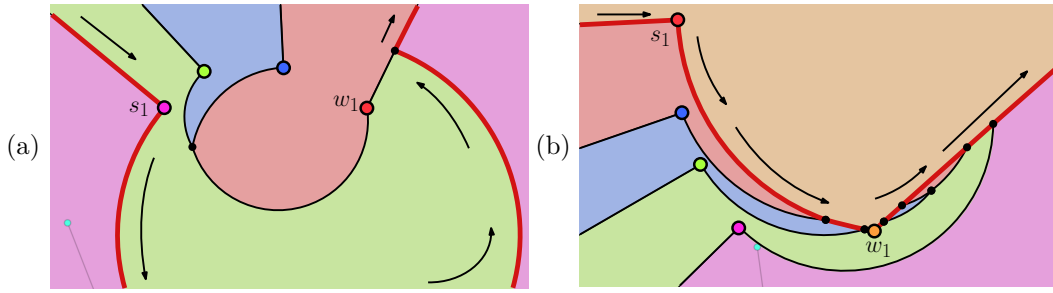
- **Tracing s_1 :** The ray s_1 lies entirely in $\text{vreg}(w_k)$. To see this, consider the set \mathcal{S}_W (before rotation) and continuously clockwise rotate all rays by an angle of $\pi/2$. During this process, w_k does not intersect any of the rays in \mathcal{S}_W , hence, $s_1 \in \text{vreg}(w_k)$. Thus, s_1 does not intersect $\text{RVD}(\mathcal{S}_W^r)$ and it can be trivially traced in $O(1)$ time.
- **Tracing E_C :** We start from the point $p(s_1)$, using the bisector $b_{\perp}(s_1, w_k)$ and we trace a chain of circular edges until we reach the ray w_1 . In order to identify at each step the next bisector to proceed, we adapt standard tracing techniques for Voronoi diagrams, see e.g., [2]. More specifically, while going from s_1 to w_1 , the curve E_C visits the regions of the sites s_1, \dots, s_l in exactly that order (some sites might possibly not appear at all). The same holds for the sites w_1, \dots, w_k but in reverse order. Hence, to trace E_C we can go over the two lists of regions in the aforementioned order.
- **Structure of E_C :** To see that the chain ends up at w_1 , consider the distance of any point on the chain to the nearest ray. The distance when the chain starts, at $p(s_1)$, is exactly $\pi/2$, and it is monotonically increasing. Moreover, consider the polygonal chain P^* consisting of the line segments $\overline{p(w_1)p(w_2)}$, $\overline{p(w_2)p(w_3)}$, \dots , $\overline{p(w_k)p(s_1)}$, $\overline{p(s_1)p(s_2)}$, \dots , $\overline{p(s_{l-1})p(s_l)}$ and the ray s_l . The distance of any point on P^* to its nearest ray, is exactly $\pi/2$. Hence, since the distance along the chain of circular edges is increasing, the chain may only end up at w_1 (but not necessarily at its apex, see e.g., Figure 9(a)).

We now need to show that the chain, which we traced, is the complete set E_C , i.e., there are no other connected components to identify. Additionally, we have to show that E_C does not induce any bounded faces in $\text{RVD}(\mathcal{S}_W^r \cup \mathcal{S}_S^r)$. To prove both statements we define an auxiliary Voronoi diagram, where in contrast to Definition 2, we define the bisector between two rays r and s , to be the entire circle $C_b(r, s)$.

We use this auxiliary diagram due to the simplicity of its bisectors. Since only the circular arcs of the bisectors appear inside P , some properties of the auxiliary Voronoi diagram also hold for $\text{RVD}(\mathcal{S}_W^r \cup \mathcal{S}_S^r)$. More specifically, each region in the auxiliary diagram is connected and the union of all the regions covers P . In addition, the auxiliary Voronoi diagram implies that $\text{RVD}(\mathcal{S}_W^r \cup \mathcal{S}_S^r)$ has $\Theta(|\mathcal{S}_W^r| + |\mathcal{S}_S^r|)$ size, hence, E_C has $O(n)$ size. The curve E_C has $O(n)$ size, and there is no backtracking while traversing the two lists of regions (to identify the edges), hence, E_C can be constructed in time $O(n)$.



■ **Figure 8** Merging diagrams (a) $\text{RVD}(\mathcal{S}_W^r)$ and (b) $\text{RVD}(\mathcal{S}_S^r)$ into (c) $\text{RVD}(\mathcal{S}_W^r \cup \mathcal{S}_S^r)$. Merging diagrams (d) $\text{RVD}(\mathcal{S}_W^r \cup \mathcal{S}_S^r)$ and (e) $\text{RVD}(\mathcal{S}_E^r \cup \mathcal{S}_N^r)$ into (f) $\text{PRVD}(\mathcal{S}_P)$. The highlighted red edges correspond to the merge curve. The arrows schematize tracing.



■ **Figure 9** Two special cases of merging two diagrams $\text{RVD}(\mathcal{S}_W^r)$ and $\text{RVD}(\mathcal{S}_S^r)$. (a) The sequence of circular edges does not end at $p(w_1)$. (b) Ray w_1 intersects $\text{RVD}(\mathcal{S}_S^r)$.

- **Tracing w_1 :** In contrast to s_1 , the ray w_1 may intersect many circular edges of $\text{RVD}(\mathcal{S}_S^r)$, each inducing a vertex; see e.g., Figure 9(b). To identify such vertices, we can intersect w_1 (starting from the point on w_1 where E_C ended) with $\text{RVD}(\mathcal{S}_S^r)$. This can be easily done in $O(\mathcal{S}_S^r)$ time, as $\text{RVD}(\mathcal{S}_S^r)$ is a tree.

All steps described can be done in $O(n)$ time, concluding the initial merging step.

Final step. We now merge $\text{RVD}(\mathcal{S}_W^r \cup \mathcal{S}_S^r)$ and $\text{RVD}(\mathcal{S}_E^r \cup \mathcal{S}_N^r)$ restricted to P . The merge curve, as it lies inside P , consists only of E_C , the set of circular edges equidistant to sites $r \in \mathcal{S}_S^r \cup \mathcal{S}_W^r$ and $t \in \mathcal{S}_E^r \cup \mathcal{S}_N^r$. Using the same properties as in the initial step, it follows that E_C consists of a single chain, it does not create bounded faces in $\text{PRVD}(\mathcal{S}_P)$, and tracing may not go outside P . Overall, E_C can be identified in $O(n)$ time, and a simple truncation of the merged diagram inside P , yields $\text{PRVD}(\mathcal{S}_P)$ in $\Theta(n)$ time, concluding the proof.

We can summarize the main result of this section as follows.

- **Theorem 15.** *Given a convex polygon P , we can construct $\text{PRVD}(\mathcal{S}_P)$ in $\Theta(n)$ time.*

4.4 Minimum angle needed to illuminate P - Brocard angle

We now turn back to the problem of computing the Brocard angle α^* of a convex polygon P . As in the respective problem in \mathbb{R}^2 , the angle α^* is realized at a point x^* on $\text{PRVD}(\mathcal{S}_P)$. Since the distance along the edges of $\text{PRVD}(\mathcal{S}_P)$ is monotone, x^* cannot lie on an edge. Further, since $\text{PRVD}(\mathcal{S}_P)$ is confined to P by definition, x^* lies actually on a vertex of $\text{PRVD}(\mathcal{S}_P)$. A special case occurs when α^* is realized by two anti-parallel rays (edges), and the circular arc of their bisector degenerates to a line segment ℓ , as in Figure 3(h). In this case, any point on ℓ is at distance α^* from the rays, but since the endpoints of ℓ are also at distance α^* , the Brocard angle is still realized at a vertex of $\text{PRVD}(\mathcal{S}_P)$.

Therefore, to find α^* we can construct $\text{PRVD}(\mathcal{S}_P)$ and then traverse it to find the vertex of maximum distance. Both steps can be done in $\Theta(n)$ time, so we obtain the following.

► **Theorem 16.** *Given a convex polygon the Brocard angle α^* can be found in $\Theta(n)$ time.*

Following, we give tight bounds on the Brocard angle.

► **Proposition 17.** *Given a convex polygon P , the Brocard angle α^* is less or equal to $\pi/2 - \pi/n$. Further, α^* can take any value in the interval $(0, \pi/2 - \pi/n]$.*

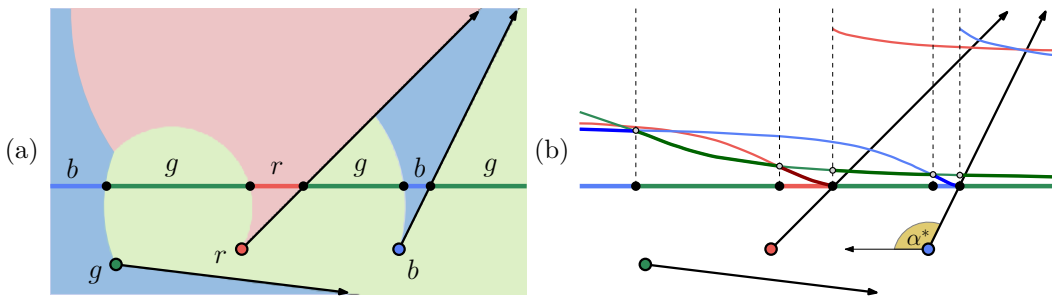
Proof. A $\pi/2 - \pi/n$ upper bound on the Brocard angle is given in [5, 12]. Such an angle is realized by regular polygons. The last illuminated point is the center of the regular polygon, which is simultaneously illuminated by all the floodlights at an angle of $\pi/2 - \pi/n$.

To prove the lower bound, consider a polygon with a bounding box of width w and height h . The aspect ratio $\frac{h}{w}$ can be arbitrarily close to zero, hence α^* is also arbitrarily close to zero. Further, we can smoothly transform any such polygon to a regular polygon, while preserving convexity. Thus, it is possible to get any Brocard angle in the range $(0, \pi/2 - \pi/n]$. ◀

As a final note, observe that the three floodlights, which realize α^* , suffice to illuminate P ; see the dashed segments in Figure 2(a). Consider the k -floodlight illumination problem [28], which asks for the minimum angle α_k , under which a convex polygon is illuminated by k floodlights, $k \geq 3$, where the sum of their apertures is α_k . The Brocard illumination gives an $\alpha_3 = 3\alpha^*$ solution to the problem. By Proposition 17, it follows that $\alpha_3 \leq 3\pi/2 - 3\pi/n$. Hence, for $n \leq 6$, the Brocard angle improves the current $a_3 = \pi$ solution given in [28].

5 RVD on curves

Floodlight illumination problems have also been considered restricted to curves. In this section, we are given a set \mathcal{S} of n rays in \mathbb{R}^2 , a set of α -floodlights each aligned with a ray, and a curve \mathcal{C} , and we want to find the minimum value of α such that \mathcal{C} is completely illuminated



■ **Figure 10** A set \mathcal{S} of 3 rays and the line $\mathcal{C} : x_2 = 0$. (a) $\text{RVD}(\mathcal{S})$ in \mathbb{R}^2 and its intersection with \mathcal{C} . (b) $\text{RVD}(\mathcal{S})$ along \mathcal{C} as the lower envelope (highlighted) of distance functions. The angle α^* is illustrated; the last illuminated point is $(-\infty, 0)$ (first illuminated by the blue ray).

by the set of α -floodlights. We show how these problems can be solved by viewing $\text{RVD}(\mathcal{S})$ as the lower envelope of distance functions in 2-space; see Figure 10. We give the proof for the case when \mathcal{C} is a line and then discuss how this approach can be extended to other curves.

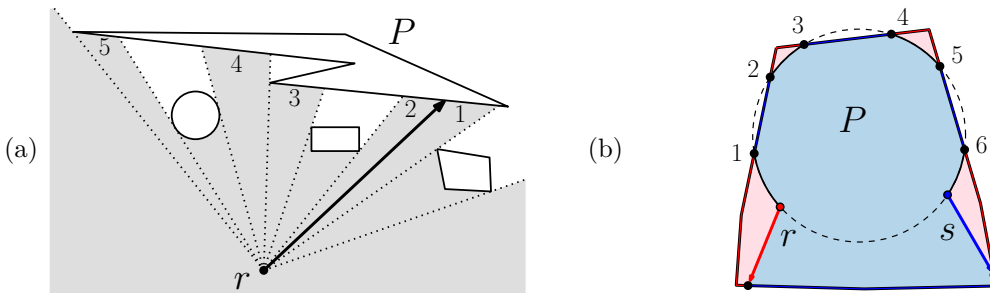
► **Theorem 18.** *Given a line \mathcal{C} , $\text{RVD}(\mathcal{S})$ along \mathcal{C} has complexity $O(n2^{\alpha(n)})$ and it can be constructed in $O(n\alpha(n) \log n)$ time.*

Proof. Without loss of generality, let \mathcal{C} be the horizontal line $x_2 = 0$. Each site $r \in \mathcal{S}$ induces a distance function which maps a point $x = (x_1, 0) \in \mathcal{C}$ to $d_{\perp}(x, r)$; see Figure 10(b). If r intersects \mathcal{C} at point $(i, 0)$, then there is a point of discontinuity, and the distance function is split into two partially defined functions, one with the domain up to i and one with the domain starting at i . $\text{RVD}(\mathcal{S})$ along \mathcal{C} is the lower envelope of these distance functions. The lower envelope of n partially defined functions, where each pair of functions intersects at most s times, has $O(\lambda_{s+2}(n))$ complexity [14] and it can be constructed in $O(\lambda_{s+1}(n) \log n)$ time [15], where $\lambda_s(n)$ is the length of the longest (n, s) Davenport-Schinzel sequence.

In our case, a pair of functions intersects at most twice, as \mathcal{C} may intersect twice the bisecting circle of the two respective rays, so $s = 2$. Further, we have at most $2n$ partially defined functions. Thus, $\text{RVD}(\mathcal{S})$ along \mathcal{C} has complexity $O(n2^{\alpha(n)})$ and it can be constructed in $O(n\alpha(n) \log n)$ time, where $\alpha(n)$ is the inverse Ackermann function. ◀

Observe that, the minimum angle α^* needed to illuminate the line \mathcal{C} is realized either at an intersection point between $\text{RVD}(\mathcal{S})$ and \mathcal{C} , or at a point of \mathcal{C} at infinity; see for example the point $(-\infty, 0)$ in Figure 10. Hence, after constructing $\text{RVD}(\mathcal{S})$ along \mathcal{C} , the angle α^* is revealed by a simple traversal of $\text{RVD}(\mathcal{S})$ in time linear in its size.

The aforementioned approach can be generalized to arbitrary curves in a straightforward way. Let \mathcal{C} be a closed curve enclosing the apices of all the rays of \mathcal{S} . Note that, if \mathcal{C} is a circle, then the same results as Theorem 18 can be derived, since \mathcal{C} intersects a bisecting circle at most twice; hence, $s = 2$. On the other hand, if \mathcal{C} is an m -sided convex polygon, then \mathcal{C} intersects a bisecting circle at most $2m$ times, hence $s = 2m$; see Figure 11(b). If \mathcal{C} is an arbitrary simple polygon, then there might be portions of \mathcal{C} not visible by a ray; thus, an additional parameter k should be introduced, to represent the number of partially defined functions corresponding to each ray.



■ **Figure 11** Illustration of the parameters s and k related to curve illumination. The boundary of the polygon P is the curve to be illuminated. (a) The distance function of the ray r is split into 5 partial functions, i.e., $k = 5$. Splits are induced by visibility constraints due to P itself (breakpoint 3-4), by visibility constraints due to other curves (breakpoint 2-3), or by the discontinuity of the distance function at the ray (breakpoint 1-2). (b) The circular arc of the bisector of the two rays r and s intersects the boundary of P at 6 points, i.e., $s = 6$.

Finally, the approach generalizes to cases where the apices of the rays are not enclosed by some curve; see Figure 11(a). As before, the complexity of $\text{RVD}(\mathcal{S})$ restricted to a curve, will be affected by a parameter s , representing the number of times a curve intersects a bisecting circle, and a parameter k , representing the number of partially defined functions in which a distance function has to be split due to visibility constraints.

6 Concluding remarks

Using the Rotating Rays Voronoi Diagram, we showed how to find the Brocard angle of a convex polygon in optimal linear time, settling an interesting open problem. We exhibited that our method is more general: given any domain D and a set of rays \mathcal{S} , we can find the minimum angle that is required to illuminate D using floodlights aligned with \mathcal{S} , by constructing $\text{RVD}(\mathcal{S})$ restricted to D .

There are many interesting questions to investigate. Regarding the Brocard angle of polygons, we would like to see how our approach could extend to other classes of polygons. We expect to have some difficulties due to the visibility constraints, but we believe that our algorithm could be adapted to work as well. Regarding $\text{RVD}(\mathcal{S})$ in \mathbb{R}^2 , we would like to settle whether the worst case combinatorial complexity is $\Theta(n^2)$. Further, if the current $O(n^{2+\epsilon})$ bound is not tight, we believe that it is possible to design $o(n^{2+\epsilon})$ -time algorithms.

References

- 1 Carlos Alegría-Galicia, David Orden, Carlos Seara, and Jorge Urrutia. Illuminating polygons by edge-aligned floodlights of uniform angle (Brocard illumination). In *Proc. European Workshop on Computational Geometry*, pages 281–284, 2017.
- 2 Franz Aurenhammer, Rolf Klein, and Der-Tsai Lee. *Voronoi Diagrams and Delaunay Triangulations*. World Scientific, 2013. URL: <http://www.worldscientific.com/worldscibooks/10.1142/8685>.
- 3 Piotr Berman, Jieun Jeong, Shiva P. Kasiviswanathan, and Bhuvan Urgaonkar. Packing to angles and sectors. In *Proc. ACM symposium on Parallel algorithms and architectures*, pages 171–180, 2007.
- 4 Arthur Bernhart. Polygons of pursuit. *Scripta Mathematica*, 24(1):23–50, 1959.
- 5 Ádám Besenyei. The Brocard angle and a geometrical gem from Dmitriev and Dynkin. *The American Mathematical Monthly*, 122(5):495–499, 2015.
- 6 Prosenjit Bose, Leonidas J. Guibas, Anna Lubiw, Mark Overmars, Diane Souvaine, and Jorge Urrutia. The floodlight problem. *International Journal of Computational Geometry & Applications*, 7(1-2):153–163, 1997.
- 7 John Casey. *A sequel to the first six books of the elements of Euclid*. Dublin University Press, 1888.
- 8 Felipe Contreras, Jurek Czyzowicz, Nicolas Fraiji, and Jorge Urrutia. Illuminating triangles and quadrilaterals with vertex floodlights. In *Proc. Canadian Conference on Computational Geometry*, 1998.
- 9 Jurek Czyzowicz, Stefan Dobrev, Benson Joeris, Evangelos Kranakis, Danny Krizanc, Jan Mañuch, Oscar Morales-Ponce, Jaroslav Opatrny, Ladislav Stacho, and Jorge Urrutia. Monitoring the plane with rotating radars. *Graphs and Combinatorics*, 31(2):393–405, 2015.
- 10 Jurek Czyzowicz, Eduardo Rivera-Campo, and Jorge Urrutia. Optimal floodlight illumination of stages. In *Proc. Canadian Conference on Computational Geometry*, pages 393–398, 1993.
- 11 Mark de Berg, Joachim Gudmundsson, Herman Haverkort, and Michael Horton. Voronoi diagrams with rotational distance costs. In *Computational Geometry Week: Young Researchers Forum*, 2017.

- 12 Nikolai A. Dmitriev and E Dynkin. On characteristic roots of stochastic matrices. *Izvestiya Rossiiskoi Akademii Nauk. Seriya Matematicheskaya*, 10(2):167–184, 1946.
- 13 Vladimir Estivill-Castro, Joseph O’Rourke, Jorge Urrutia, and Dianna Xu. Illumination of polygons with vertex lights. *Information Processing Letters*, 56(1):9–13, 1995.
- 14 Sergiu Hart and Micha Sharir. Nonlinearity of Davenport—Schinzel sequences and of generalized path compression schemes. *Combinatorica*, 6(2):151–177, 1986.
- 15 John Hershberger. Finding the upper envelope of n line segments in $O(n \log n)$ time. *Information Processing Letters*, 33(4):169–174, 1989.
- 16 Dan Ismailescu. Illuminating a convex polygon with vertex lights. *Periodica Mathematica Hungarica*, 57(2):177–184, 2008.
- 17 Rolf Klein. *Concrete and Abstract Voronoi diagrams*, volume 400. Springer Science & Business Media, 1989.
- 18 Rolf Klein, Elmar Langetepe, and Zahra Nilforoushan. Abstract Voronoi diagrams revisited. *Computational Geometry: Theory and Applications*, 42(9):885–902, 2009.
- 19 Rolf Klein and Andrzej Lingas. Hamiltonian abstract Voronoi diagrams in linear time. In *Proc. International Symposium on Algorithms and Computation*, pages 11–19, 1994.
- 20 Evangelos Kranakis, Danny Krizanc, and Oscar Morales. Maintaining connectivity in sensor networks using directional antennae. In *Theoretical Aspects of Distributed Computing in Sensor Networks*, pages 59–84. Springer, 2011.
- 21 Azin Neishaboori, Ahmed Saeed, Khaled A. Harras, and Amr Mohamed. On target coverage in mobile visual sensor networks. In *Proc. ACM International Symposium on Mobility Management and Wireless Access*, pages 39–46, 2014.
- 22 Joseph O’Rourke. Visibility. In *Handbook of discrete and computational geometry*, pages 875–896. CRC Press, 2017.
- 23 Joseph O’Rourke, Thomas Shermer, and Ileana Streinu. Illuminating convex polygons with vertex floodlights. In *Proc. Canadian Conference on Computational Geometry*, pages 151–156, 1995.
- 24 Micha Sharir. Almost tight upper bounds for lower envelopes in higher dimensions. *Discrete & Computational Geometry*, 12(3):327–345, 1994.
- 25 William Steiger and Ileana Streinu. Illumination by floodlights. *Computational Geometry*, 10(1):57–70, 1998.
- 26 Tsuyoshi Taki, Jun-ichi Hasegawa, and Teruo Fukumura. Development of motion analysis system for quantitative evaluation of teamwork in soccer games. In *Proc. IEEE International Conference on Image Processing*, volume 3, pages 815–818. IEEE, 1996.
- 27 Csaba D. Tóth. Art galleries with guards of uniform range of vision. *Computational Geometry*, 21(3):185–192, 2002.
- 28 Jorge Urrutia. Art gallery and illumination problems. In *Handbook of Computational Geometry*, pages 973–1027. Elsevier, 2000.